

# BEAM OPTICS OF 180-DEGREE BENDING SECTION INCLUDING A CHARGE STRIPPER\*

Ji-Ho Jang<sup>#</sup>, Hyun-Chang Jin, Jeong-Seog Song, RISP/IBS, Daejeon, Korea

## Abstract

The linac of RISP (Rare Isotope Science Project) [1, 2] includes a charge stripper in order to obtain better acceleration efficiency. It is located after the lower energy part of the superconducting linac which accelerates 2 charge states, 33 and 34 of uranium beams to about 18 MeV/u. After the charge stripper, 5 charge states around 79 are selected and transported into the higher energy part of the linac through a 180-degree bending section called P2DT. This work focused on the beam optics result by using DYNAC code [3] and compared with TRACK [4] simulation. It also includes the charge stripper effects on the beam optics in the 180-degree bending section.

## INTRODUCTION

The 180-degree bending section in RISP linac was designed by using the 2<sup>nd</sup> order achromatic and isochronous principles [5]. It includes 2 collimators in order select 5 charge states of the uranium beams among several charge states produced in the charge stripper. The halo particles will be removed in several slits located after the charge stripper.

We are considering the DYNAC code as our online model because the simulation with multiple charge states is possible, and it is fast enough and gives consistent results to TRACK in the simulations of the LEBT and SCL sections [6]. The beam specification of RISP linac is summarized in Table 1. We focused on the uranium beam in this study.

Table 1: Beam Specification for the RISP Linac

Parameters	H <sup>+</sup>	O <sup>8+</sup>	Xe <sup>54+</sup>	U <sup>79+</sup>
Energy [MeV/u]	600	320	251	200
Current [pμA]	660	78	11	8.3
Power on target [kW]	>400	400	400	400

## CHARGE STRIPPER

We studied the change of the particle distribution in the charge stripper by using SRIM code [7] and compared the results with TRACK simulation. We also studied beam optics through the 180-degree bending section after carbon stripper [8]. In this section, we summarized the

charge stripper effects especially on kinetic energy.

The energy reduction in a carbon stripper of the thickness of 1mg/cm<sup>2</sup> is obtained by using SRIM code. We varied the input kinetic energy of uranium beams from 17 MeV/u to 20 MeV/u. The lower energy part of RISP linac will produce the beam energy of about 18 MeV/u. The result is given in Fig. 1. The energy reduction is about 0.47 MeV/u in the case of the 18 MeV/u input energy. We also compared the output kinetic energy with the Bethe-Bloch formula [9]. The result is shown in Fig. 2 [8]. We found that the difference is about 1.6 % for the input energy of 17 MeV/u and about 1.1% for 20 MeV/u. The SRIM value of the kinetic energy reduction in the carbon stripper was used for the TRACK simulation of the 180-degree bending section. The Bethe-Bloch formula was used to estimate the energy reduction through the carbon stripper in DYNAC simulation.

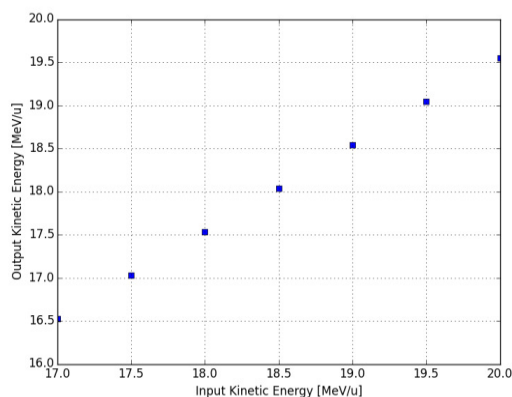


Figure 1: SRIM results of output kinetic energy after the carbon stripper depending on input kinetic energy.

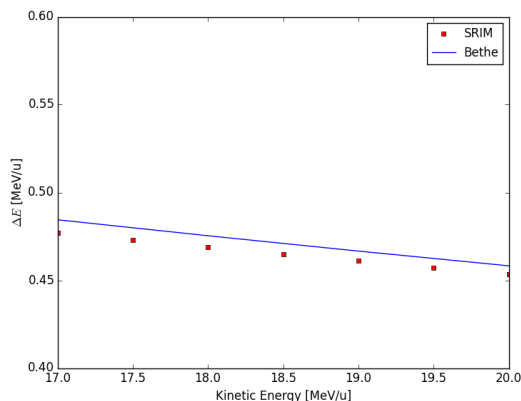


Figure 2: Energy reduction in SRIM simulation compared with the Bethe-Bloch formula in the carbon stripper.

\*Work supported by Ministry of Science, ICT and Future Planning  
#jhjang@ibs.re.kr

### 180-DEGREE BENDING SECTION

The 180-degree bending section consists of 4 45-degree bending magnets, 18 quadrupole magnets, 8 sextupole magnets for 2<sup>nd</sup> order achromatic condition, 2 rebuncher cavities to control the longitudinal beam properties, and 2 collimators for charge selection. In the following simulation, we used a single charge state of 33 with kinetic energy of 18 MeV/u at the end of the lower energy part of the linac.

Figure 3 shows the kinetic energy result of DYNAC through the bending section. We used the Bethe-Bloch formula [9]:

$$\left\langle -\frac{dE}{dx} \right\rangle = 4\pi N_A r_e^2 m_e c^2 z^2 \frac{Z}{A\beta^2} \left[ \frac{1}{2} \ln \frac{2m_e c^2 \beta^2 \gamma^2 T_{max}}{I^2} - \beta^2 - \frac{C}{Z} - \frac{\delta}{2} \right],$$

where the details of each terms can be found in Ref. [9]. We found the DYNAC result with Bethe-Bloch formula is consistent with the TRACK simulation.

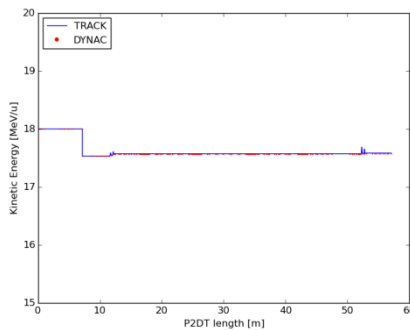


Figure 3: Kinetic energy change in the 180-degree bending section with TRACK and DYNAC.

We compared the particle distribution after the charge stripper between TRACK and DYNAC codes. Figure 4 shows the particle distribution after the charge stripper in phase spaces. Figs. 5 and 6 show the particle distribution in x' and y' spaces. They also include the Gaussian fitting curve for each case. We note that the distributions are slightly different between two codes.

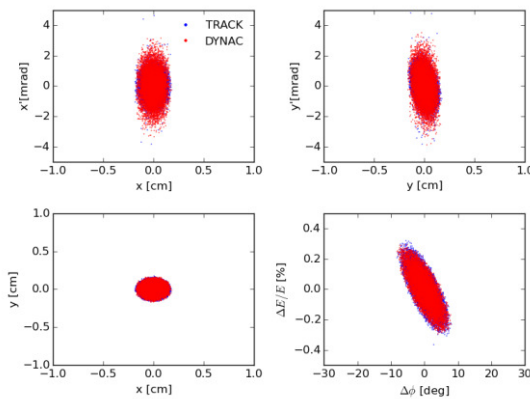


Figure 4: Particle distribution after the carbon stripper in phase spaces with TRACK and DYNAC.

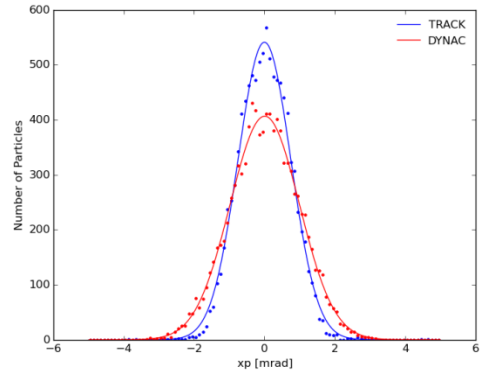


Figure 5: Particle distribution after the carbon stripper in x' space with TRACK and DYNAC.

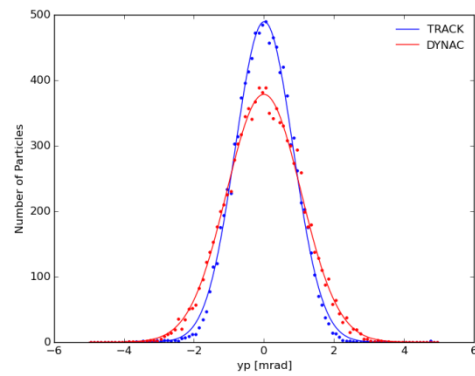


Figure 6: Particle distribution after the carbon stripper in y' space with TRACK and DYNAC.

Figures 7 and 8 show the particle distribution after the 1<sup>st</sup> and 2<sup>nd</sup> collimators in phase spaces. The particle distributions in horizontal direction are given in Fig. 9 and Fig. 10. In the first collimator, we can partially eliminate the charge states ≤ 76 and ≥ 82 because each charge state is not clearly separated. The complete charge selection can be achieved in the 2<sup>nd</sup> collimator.

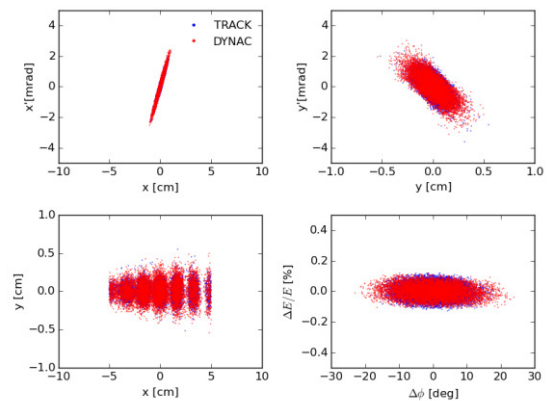


Figure 7: Particle distribution after the 1<sup>st</sup> collimator in phase spaces with TRACK and DYNAC.

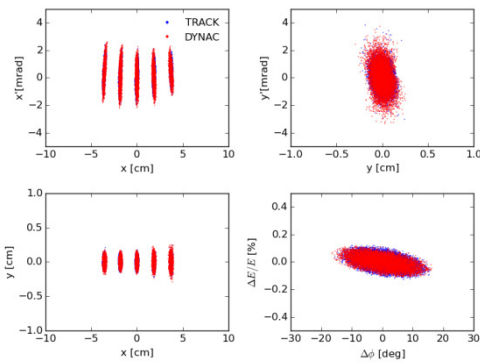


Figure 8: Particle distribution after the 2<sup>nd</sup> collimator in phase spaces with TRACK and DYNAC.

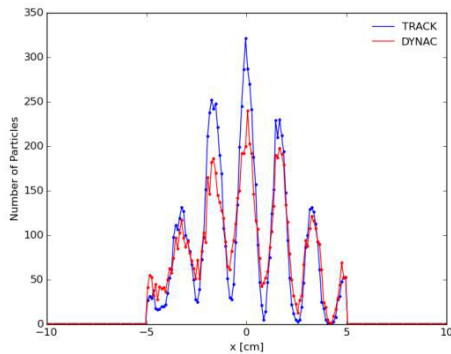


Figure 9: Particle distribution after the 1<sup>st</sup> collimator in the horizontal direction with TRACK and DYNAC.

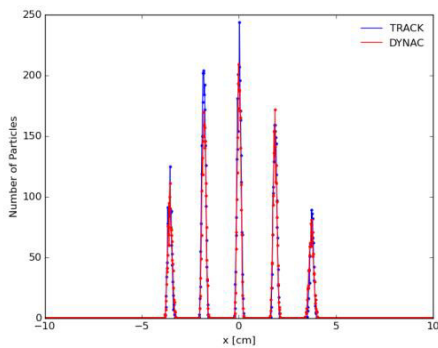


Figure 10: Particle distribution after the 2<sup>nd</sup> collimator in the horizontal direction with TRACK and DYNAC.

Figure 11 shows the rms envelope through the bending section. We found that the results with TRACK and DYNAC are consistent with each other and the difference in particle distributions in Figs. 5 and 6 is not important. The particle distribution in phase space is given in Fig. 12 at the end of the bending section.

In conclusion, we studied the kinetic energy reduction in the charge stripper with SRIM code. We also studied beam optics in the 180-degree bending section with DYNAC code and compared with TRACK results. We

found that DYNAC results are consistent with TRACK simulation.

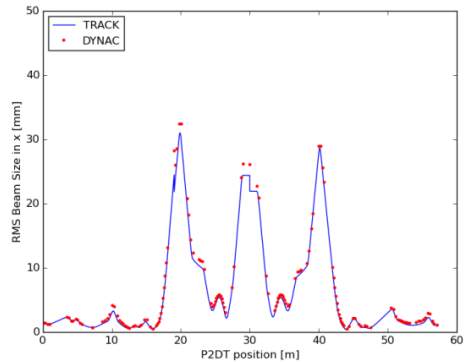


Figure 11: rms beam envelope through the bending section with TRACK and DYNAC simulations.

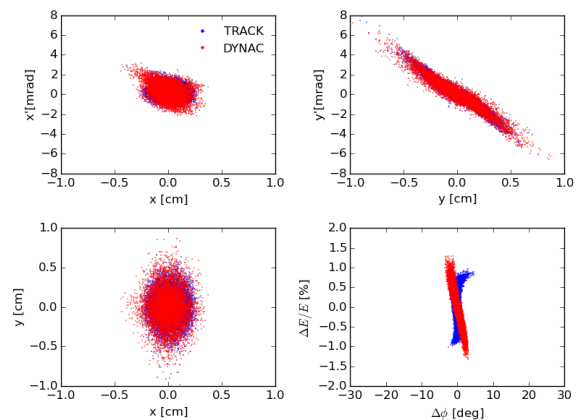


Figure 12: Particle distribution at the end of the bending section with TRACK and DYNAC simulations.

## REFERENCES

- [1] D. Jeon *et al.*, J. Korean Phys. Soc. 65, 1010 (2014).
- [2] J. H. Jang *et al.*, “Beam Physics Challenges in RAON”, HB 2014, East-Lansing, p. 226 (2014); <http://www.JACoW.org>.
- [3] L. Lapostolle *et al.*, “Program DYNAC: User Guide (ver. 6)”; <http://dynac.web.cern.ch/dynac/dynac.html>
- [4] P.N. Ostroumov *et al.*, TRACK, ANL Technical Note, Updated for version 3.7.
- [5] H. C. Jin, *et al.*, Nucl. Instrum. Methods. Phys. Res. A795, 65 (2015).
- [6] J. H. Jang *et al.*, “Beam Optics of RISP Linac using DYNAC code”, IPAC2015, Richmond, p. 3845 (2015); <http://www.JACoW.org>
- [7] Website for SRIM code: <http://www.srim.org/>.
- [8] J.H. Jang *et al.*, “Charge Stripper Effects on Beam Optics in 180-degree Bending Section of RISP Linac”, ICABU 2015, Gyeongju (2015). The results were submitted to JKPS.
- [9] D. Groom, Particle Data Group Notes, PDG-93-06, 8 December 1993.